Supplementary Information: Controlling the Spin-orbit Branching Fraction in Molecular Collisions

Cornelia G. Heid,[†] Imogen P. Bentham,[†] Victoria Walpole,[†,§] Pablo G. Jambrina,[‡] F. Javier Aoiz,[¶] and Mark Brouard[*,†]

[†]*Department of Chemistry, University of Oxford, The Chemistry Research Laboratory, 12 Mansfield Road, Oxford, OX1 3TA, United Kingdom*

[‡]*Departamento de Química Física, Universidad de Salamanca, 37008, Salamanca, Spain*

[¶]*Departamento de Química Física, Facultad de Química, Universidad Complutense, 28040 Madrid, Spain*

[§]*Current address: Max Planck Institute for Biophysical Chemistry, Am Faßberg 11, 37077 Göttingen, Germany*

E-mail: mark.brouard@chem.ox.ac.uk.

November 9, 2020

Methods

Computational Methods

The quantum mechanical (QM) theory to calculate the differential cross sections (DCSs) and bond-axis polarization dependent differential cross sections (r-PDDCSs, $R_q^{(k)}(\theta)$) for any arbitrary orientation of the collision partners has been described in refs. 1 and 2. Close-coupled QM scattering calculations were carried out with the Hibridon suite of codes,[3] on the potential energy surfaces (PESs) of Alexander.[4,5] Rotational states up to $j' = 20.5$, both spin-orbit manifolds ($|\Omega| = \frac{1}{2}, \frac{3}{2}$) and both Λ-doublet levels (e, f) were included in the scattering calculations. A total of $J = 190$ partial waves were used to ensure convergence. To account for the spread in the experimental collision energy, the calculations were run at seven different collision energies ranging from 590 cm^{-1} to 710 cm^{-1}, with a spacing of 20 cm^{-1}. The results were weighted and averaged over a Gaussian distribution function, with a mean of 651 cm^{-1} and a FWHM of 35 cm^{-1}.

The superposition state of the NO molecules in the orientation field consists of the initial e and f wave functions:[6–8]

$$|jm_E|\Omega|E\rangle = \frac{1}{\sqrt{2}}\left[\alpha(E)\,|jm_E|\Omega|e\rangle + \beta(E)\,|jm_E|\Omega|f\rangle\right] , \tag{S.1}$$

where m_E designates the projection of j onto the electric field vector, $\boldsymbol{E}$, and $\alpha(E)$ and $\beta(E)$ are the field-dependent mixing parameters,

$$|\alpha(E)| = \sqrt{1 - \frac{1}{\sqrt{1+E_{\mathrm{red}}^2}}} \qquad \text{and} \qquad |\beta(E)| = \sqrt{1 + \frac{1}{\sqrt{1+E_{\mathrm{red}}^2}}} , \tag{S.2}$$

such that $\alpha(E)^2 + \beta(E)^2 = 2$.[6,7] The strength of the reduced electric field is defined as:

$$E_{\mathrm{red}} = \frac{2W_{\mathrm{stark}}}{E_\Lambda} , \tag{S.3}$$

with W_{stark} denoting the linear Stark effect and E_Λ the Λ-doublet splitting. At the electric field

strength used in our experiments, $|\alpha| = 0.64$ and $|\beta| = 1.26$.

The r-PDDCSs (for $j = \frac{1}{2}$) were calculated using these values for α and β and the scattering amplitudes, $F_{m'\varepsilon' m\varepsilon} \equiv f_{j'\Omega' m'\varepsilon' \leftarrow j\Omega m\varepsilon}(\theta)$, obtained in the Hibridon calculations,[1,2,9]

$$\frac{\sigma_{\rm iso}}{2\pi} R_0^{(0)}(\theta) = \frac{1}{2}(\alpha^2 Q_{1/2e\,1/2e} + \beta^2 Q_{1/2f\,1/2f}) \quad \text{(S.4)}$$

$$\frac{\sigma_{\rm iso}}{2\pi} R_0^{(1)}(\theta) = \frac{1}{2}(Q_{1/2f\,1/2e} + Q_{1/2e\,1/2f}) \quad \text{(S.5)}$$

$$\frac{\sigma_{\rm iso}}{2\pi} R_1^{(1)}(\theta) = -\frac{1}{2\sqrt{2}}(Q_{-1/2f\,1/2e} + Q_{1/2e\,-1/2f}) \,, \quad \text{(S.6)}$$

where, for given initial j, Ω and final j', Ω', ε',

$$Q_{m_1\varepsilon_1 m_2\varepsilon_2} \equiv \sum_{m'} F_{m'\varepsilon' m_1\varepsilon_1} F^*_{m'\varepsilon' m_2\varepsilon_2} \,, \quad \text{(S.7)}$$

and m and m' designate the projections of j and j' onto the relative velocity vector, $\boldsymbol{k}$, and ε and ε' are the symmetry indices of the initial and final states, respectively. $\sigma_{\rm iso}$ is the isotropic integral cross section in the presence of a field.

The $R_q^{(k)}(\theta)$ moments were then substituted into eq (2) (in the main text) to calculate the differential cross sections for orientations in the entire range of $\theta_E = 0^\circ - 180^\circ$ (with $\phi_E = 0^\circ$ and $\phi_E = 180^\circ$), using a step size of 0.5°. The differential branching fraction was calculated according to eq (3). For the integral branching fractions, the DCSs were integrated over $\cos\theta$ at each $\theta_E/\phi_E = 0^\circ$ and $\theta_E/\phi_E = 180^\circ$ point, and the resulting integral cross sections (ICSs) substituted into eq (9). Note that the $R_0^{(0)}(\theta)$ moment is simply the isotropic normalized differential cross section such that its integral over $\cos\theta$ is $r_0^{(0)} = 1$.

Experimental Methods

In the experiment, hexapole state selection was combined with electric field orientation to define the initial quantum state of the NO molecules and their spatial arrangement relative to the incoming Ar atoms. A set of four rods, two of which had a positive charge of 8 kV and two of which had a

negative charge of -8 kV applied to them, was used to create the orientation field. The rods were mounted on a rotatable stage, which provides access to any arbitrary initial collision geometry. The scattering distributions for a specific initial orientation and a specific final rotational state were recorded using velocity-map ion imaging, during which all four rods were switched to about 1 kV, using Behlke switches. A full description of the experimental methods can be found in refs. 1 and 2.

The extraction of the experimental *r*-PDDCSs has been described in detail in our earlier work for the side-on orientation,[1,2] and the $R_0^{(0)}(\theta)$ and $R_1^{(1)}(\theta)$ moments, shown in Fig. 2 of the main text, are from our earlier measurements in the spin-orbit conserving[2] and changing[9] manifolds. Briefly, the experimental velocity-map ion images for the two side-on orientations were added and fitted to a set of modified spherical harmonics basis functions to extract the $R_0^{(0)}(\theta)$ moment. An analogous procedure was used to fit the difference image and obtain the $R_1^{(1)}(\theta)$ moment. The error of the experimentally determined $R_0^{(0)}(\theta)$ and $R_1^{(1)}(\theta)$ moments were calculated from the variance of the fits to the whole and the slow and fast sides of each sum and difference image.

The experimental integral branching fractions were obtained from the integral steric asymmetries (ISAs), S_x and S_z, measured previously for the side-on ($\pm x$) and end-on ($\pm z$) orientations, respectively, in both spin-orbit manifolds ($\Delta\Omega = 0, \Delta\Omega = 1$).[2,9–11] The ISAs are defined as:

$$S_x = \frac{\sigma_{+x} - \sigma_{-x}}{\sigma_{+x} + \sigma_{-x}} = \frac{\sigma_{90^\circ}^{0^\circ} - \sigma_{90^\circ}^{180^\circ}}{\sigma_{90^\circ}^{0^\circ} + \sigma_{90^\circ}^{180^\circ}} \tag{S.8}$$

and

$$S_z = \frac{\sigma_{-z} - \sigma_{+z}}{\sigma_{+z} + \sigma_{-z}} = \frac{\sigma_{180^\circ}^{\phi_E} - \sigma_{0^\circ}^{\phi_E}}{\sigma_{180^\circ}^{\phi_E} + \sigma_{0^\circ}^{\phi_E}}\,, \tag{S.9}$$

with $\sigma_{\pm x/z}$ denoting the ICS for the indicated orientation. The errors were propagated from the error in the S_x and S_z values. The mean collision energy in the side-on experiments[2,9] and the end-on spin-orbit changing measurements[11] was 651 cm^{-1}, while the end-on spin-orbit conserving measurements used a mean collision energy of 530 cm^{-1}.[10] The QM calculated ISAs for the two collision energies show only minor deviations in the range of final states considered in this

work. The deviations are insignificant compared to the uncertainty associated with the experimental measurement and were therefore neglected in the error propagation.

Spin-orbit Branching Fractions for Isotropic Distributions

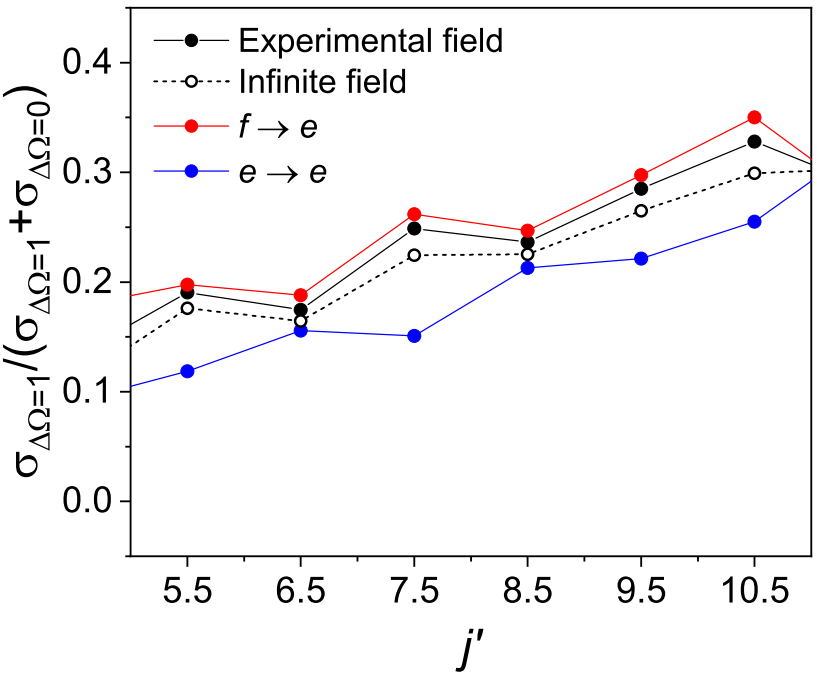

Figure S 1: Integral spin-orbit fractions for the isotropic distributions at the experimental (full black circles) and at infinite (open black circles) field strength, and for the pu re $f \rightarrow e$ (red) and $e \rightarrow e$ (blue) transitions in the absence of a field. The fractions are plotted as a function of final e Λ-doublet state.

The isotropic cross section in the static electric field, σ_{iso}, corresponds to orientation along the y-axis, with $S_y = 0$. Figure S1 compares the calculated integral spin-orbit branching fractions for an isotropic distribution in the presence and in the absence of an electric field. The full and open black circles represent the spin-orbit branching fractions at the experimental and at infinite field strengths, respectively, while the red and blue traces correspond to the fractions for the pure $f \rightarrow e$ and $e \rightarrow e$ transitions without a field.[12] In the presence of the orienting field, the relative contributions of the e and f states to the initial mixed state is given by the field-dependent $\alpha(E)$

and $\beta\,(E)$ coefficients, as shown above in eq (S.1). At the experimental field strength, the latter coefficient is about twice as large as the former, indicating a prevalence of the f-state contribution to the mixed initial state. Thus, at the experimental field, we can roughly compare the isotropic branching fraction (expressed in terms of the isotropic cross sections, $\sigma_{\rm iso}$) for a particular final state with the branching fraction calculated for the $f \rightarrow e$ transition in the absence of a field. The figure shows that the isotropic spin-orbit branching fractions are somewhat field-dependent, reflecting the varying contributions of the field-free e and f levels to the initial mixed state. At infinite field, where the two f and e states contribute equally to the initial mixed state, the spin-orbit branching fractions are more of an equal mix of the two pure transitions.

References

(1) Heid, C. G.; Walpole, V.; Brouard, M.; Aoiz, F. J.; Jambrina, P. G. Side-impact collisions of Ar with NO. *Nat. Chem.* **2019**, *11*, 662–668.

(2) Walpole, V.; Heid, C. G.; Jambrina, P. G.; Aoiz, F. J.; Brouard, M. Steric effects in the inelastic scattering of NO(X) + Ar: Side-on orientation. *J. Phys. Chem. A* **2019**, *123*, 8787–8806.

(3) HIBRIDON is a package of programs for the time-independent quantum treatment of inelastic collisions and photodissociation written by M. H. Alexander, D. E. Manolopoulos, H. Werner and B. Follmeg, with contributions by P. F. Vohralik, D. Lemoine, G. Corey, R. Gordon, B. Johnson, T. Orlikowski, A. Berning, A. D. Esposti, C. Rist, P. Dagdigian, B. Pouilly, G. van der Sanden, M. Yang, F. de Weerd, S. Gregurick and J. Kłos.

(4) Alexander, M. H. A new, fully *ab initio* investigation of the NO($X^2\Pi$) Ar system. I. Potential energy surfaces and inelastic scattering. *J. Chem. Phys.* **1999**, *111*, 7426–7434.

(5) Alexander, M. H. A new, fully *ab initio* investigation of the ArNO($X^2\Pi$) system. II. Bound states of the Ar–NO complex. *J. Chem. Phys.* **1999**, *111*, 7435–7439.

(6) van Leuken, J.; Bulthuis, J.; Stolte, S.; Snijders, J. Steric asymmetry in rotationally inelastic state-resolved NO-Ar collisions. *Chem. Phys. Lett.* **1996**, *260*, 595–603.

(7) de Lange, M.; Drabbels, M.; Griffiths, P.; Bulthuis, J.; Stolte, S.; Snijders, J. Steric asymmetry in state-resolved NO–Ar collisions. *Chem. Phys. Lett.* **1999**, *313*, 491–498.

(8) Alexander, M. H.; Stolte, S. Investigation of steric effects in inelastic collisions of NO($X^2\Pi$) with Ar. *J. Chem. Phys.* **2000**, *112*, 8017–8026.

(9) Heid, C. G.; Bentham, I. P.; Walpole, V.; Gheorghe, R.; Jambrina, P. G.; Aoiz, F. J.; Brouard, M. Probing the location of the unpaired electron in spin-orbit changing collisions of NO with Ar. *Phys. Chem. Chem. Phys.* **2020**, *22*, 22289–22301.

(10) Nichols, B.; Chadwick, H.; Gordon, S. D. S.; Eyles, C. J.; Hornung, B.; Brouard, M.; Alexander, M. H.; Aoiz, F. J.; Gijsbertsen, A.; Stolte, S. Steric effects and quantum interference in the inelastic scattering of NO(X) + Ar. *Chem. Sci.* **2015**, *6*, 2202–2210.

(11) Brouard, M.; Gordon, S. D. S.; Hackett Boyle, A.; Heid, C. G.; Nichols, B.; Walpole, V.; Aoiz, F. J.; Stolte, S. Integral steric asymmetry in the inelastic scattering of NO($X^2\Pi$). *J. Chem. Phys.* **2017**, *146*, 014302.

(12) Alexander, M. H. Differential and integral cross sections for the inelastic scattering of NO($X^2\Pi$) by Ar based on a new *ab initio* potential energy surface. *J. Chem. Phys.* **1993**, *99*, 7725–7738.